NGU REPORT 2022.008

Helicopter-borne magnetic, electro-magnetic and radiometric geophysical survey in Trøndelag area, Trøndelag County

GEOLOGY FOR SOCIETY

SINCE 1858

GEOLOGICAL SURVEY OF NORWAY

- NGU -

NGU REPORT
2022.008

Helicopter-borne magnetic, electro-magnetic and radiometric geophysical survey in Trøndelag area, Trøndelag County

NORGES GEOLOGISKE UNDERSØKELSE
- NGU -

REPORT

Geological Survey of Norway
P.O.Box 6315 TORGARDEN
NO-7491 TRONDHEIM
Tel.: 47 73 90 40 00

Report no.: 2022.008

ISSN: 0800-3416 (print)
ISSN: 2387-3515 (online)

Grading: Open

Title: Helicopter-borne magnetic, electromagnetic and radiometric geophysical survey in Trøndelag area, Trøndelag County.

Authors:
Frida Mathayo Mrope, Alexandros Stampolidis, Marie-Andrée Dumais, Frode Ofstad, Tom Kristiansen and Georgios Tassis

Client:
NGU

County:
Trøndelag

Municipality:
Stjørdal, Selbu, Malvik and Meråker

Map-sheet name (M=1:250.000)
Trondheim

Map-sheet no. and -name (M=1:50.000)
1721-IV Flornes,1721-III Tydal,1722-III Levanger

Deposit name and grid-reference:
WGS84 UTM32N 615000E, 7030000N

Number of pages: 35 **Price (NOK):** 125
Map enclosures:

Fieldwork carried out:	**Date of report:**	**Project no.:**	**Person responsible:**
July 2021	March 2022	388900	Marco Brönner

Summary:

NGU conducted an airborne geophysical survey in Stjørdal, Selbu, Malvik and Meråker municipalities, as part of NGU's general airborne mapping program.

This report describes and documents the acquisition, processing and visualization of the acquired datasets and presents them in maps. The geophysical surveys consist of 2655 line-km data, covering an area of 535 km^2 flown on July 21st to 29th 2021 and August 30th to September 6th 2021.

The NGU modified Geotech Ltd. Hummingbird frequency domain electromagnetic system supplemented by an optically pumped Cesium magnetometer and the Radiation Solutions 1024 channels RSX-5 spectrometer mounted on a AS350-B3 helicopter was used for data acquisition.

The survey was flown with 200 meters line spacing, azimuth 100º. The average speed was 106 km/h, and the average height clearance of the bird was 45.7 m for the magnetometer and electromagnetic probe and 75.7 m for the spectrometer.

Collected data were processed at NGU using Geosoft Oasis Montaj software. Raw total magnetic field data were corrected for diurnal variation and levelled using Geosoft micro-levelling algorithm. Radiometric data were processed using standard procedures as recommended by International Atomic Energy Association (IAEA).

The electromagnetic data were filtered and levelled using both automated and manual levelling procedures. The apparent resistivity was calculated from in-phase and quadrature data for three coplanar frequencies (880 Hz, 6600 Hz and 34133 Hz), and for two coaxial frequencies (980 Hz and 7000 Hz).

All data were gridded using cell size of 50 m x 50 m and presented as 40% transparent grids with shaded relief on top of topographic maps. The electromagnetic data are presented as 30% transparent grids on top of topographic maps.

Keywords:	**Airborne**	**Geophysics**
Magnetic	**Gamma-ray spectrometry**	**Radiometric**
Electromagnetic	**Technical report**	

CONTENTS

1. INTRODUCTION 6
2. SURVEY SPECIFICATIONS 7
2.1 Airborne Survey Parameters 7
2.2 Airborne Survey Instrumentation 8
2.3 Airborne Survey Logistics Summary 9
3. DATA PROCESSING AND PRESENTATION 10
3.1 Total Field Magnetic Data 10
3.2 Electromagnetic Data 12
3.3 Radiometric data 13
4. PRODUCTS 17
5. REFERENCES 18
Appendix A1: Flow chart of magnetic processing 19
Appendix A2: Flow chart of EM processing 19
Appendix A3: Flow chart of radiometry processing 19

FIGURES

Figure 1: Helicopter survey area in Trøndelag. 6
Figure 2: Hummingbird system in air. 8
Figure 3: Gamma-ray spectrum with K, Th, U and Total Count windows. 13
Figure 4: Trøndelag survey area with flight paths. 21
Figure 5: Total Magnetic Field. 22
Figure 6: Magnetic Horizontal Gradient. 23
Figure 7: Magnetic Vertical Gradient. 24
Figure 8: Magnetic Tilt Derivative. 25
Figure 9: Apparent resistivity. Frequency 7000 Hz, Coaxial coils. 26
Figure 10: Apparent resistivity. Frequency 6600 Hz, Coplanar coils. 27
Figure 11: Apparent resistivity. Frequency 980 Hz, Coaxial coils. 28
Figure 12: Apparent resistivity. Frequency 880 Hz, Coplanar coils. 29
Figure 13 Apparent resistivity. Frequency 34133 Hz, Coplanar coils. 30
Figure 14: Radiometric Total counts. 31
Figure 15: Potassium ground concentration. 32
Figure 16: Uranium ground concentration. 33
Figure 17: Thorium ground concentration. 34
Figure 18: Radiometric Ternary Image. 35

TABLES

Table 1. Flight specifications 6
Table 2. Instrument Specifications 8
Table 3. Hummingbird EM system, frequency, and coil configurations 9
Table 4. Survey Specifications Summary 9
Table 5. Specified channel windows for the 1024 RSX-5 system. 13
Table 6. Maps available from NGU on request. 17

1. INTRODUCTION

In 2021 NGU received government funds to acquire airborne geophysical data from parts of Trøndelag county. The surveyed area is situated between Stjørdal to the left and Meråker to the right. The helicopter survey reported herein amounts to 2655 line-km, or 535 km^2, with the area covered shown in Figure 1. The survey area is marked with a red border and was flown from the 21st to 29th of July and 30th of August to 6th of September 2021.

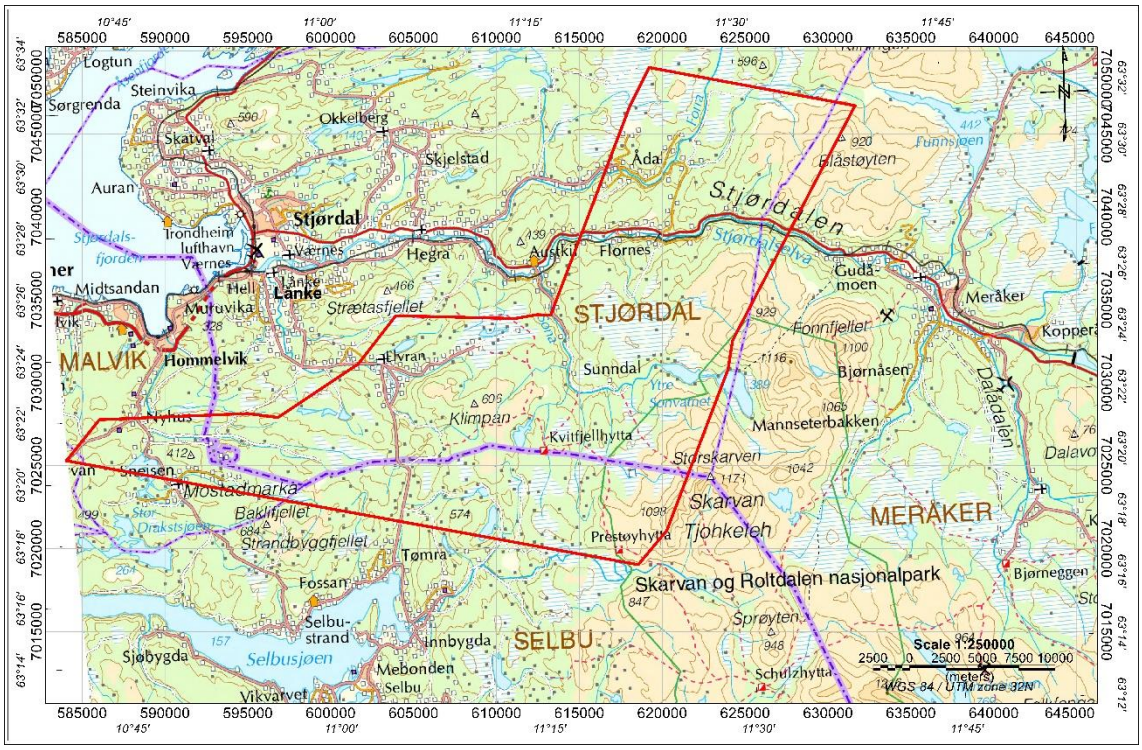

Figure 1: Helicopter survey area in Trøndelag.

Table 1. Flight specifications

Survey Name	Surveyed lines (km)	Surveyed area (Km^2)	Line direction	Average flight speed (km/h)
Trøndelag 2021	2655	535	100^o	106

The objective of the airborne geophysical survey was to obtain a dense high-resolution magnetic, electromagnetic and radiometric dataset over the survey area. This data is required for the enhancement of a general understanding of the regional geology of the area, with adjoining areas covered by other airborne surveys in earlier years.

In this regard, the new data can be used to map contacts and structural features within the survey area. It also improves defining the potential of known zones of mineralization, their geological settings, and identifying new areas of interest, as the dataset fills a gap in the high-resolution geophysical surveys of the region.

The survey incorporated the use of a Hummingbird™ 5-frequency electromagnetic (EM) system supplemented by a high-sensitivity Cesium magnetometer, gamma-ray spectrometer, and radar altimeter. A GPS navigation computer system with flight path indicators ensured accurate positioning of the geophysical data with respect to the World Geodetic System 1984 geodetic datum (WGS-84).

2. SURVEY SPECIFICATIONS

2.1 Airborne Survey Parameters

NGU used a modified Hummingbird™ electromagnetic and magnetic helicopter survey system designed to obtain low level, slow speed, detailed airborne magnetic and electromagnetic data (Geotech 1997). The system was supplemented by 1024-channel gamma-ray spectrometer, installed under the belly of the helicopter, which was used to acquire the radiometric data and map the ground concentrations of Uranium (U), Thorium (Th) and Potassium (K), and radiation Total Counts.

A Eurocopter AS350-B3 (LN-OSD) owned by the helicopter company Pegasus Helicopter AS was used to tow the bird. The survey lines were spaced 200 meters apart and oriented at 100°. The magnetic and electromagnetic sensors are housed in a single 7-meter-long bird, flown at an average of 45.7 m above the topographic surface.

Rugged terrain and abrupt changes in topography affected the aircraft pilot's ability to 'drape' the terrain, meaning the average instrumental height was sometimes higher than the standard survey instrumental height, which is defined as 30 meters plus a height of obstacles (trees, power lines etc.) for the electromagnetic and magnetic sensors.

The ground speed of the aircraft varied from 65 – 130 km/h depending on topography, wind direction and its magnitude. On average the ground speed during measurements is calculated to 106 km/h. The magnetic data were recorded at 0.2 second intervals resulting in approximately 6 meters average point spacing.

The electromagnetic data were recorded at 0.1 second intervals resulting in data with a sample increment of 3 meters along the ground in average. The radiometric data were recorded at every 1 second giving a point spacing of approximately 29.4 meters. The above parameters allow recognizing sufficient details in the data to detect subtle anomalies that may represent mineralization and/or rocks of different lithological and petrophysical composition.

A base station magnetometer to monitor diurnal variations in the magnetic field was located at the base in Lånke in Stjørdal municipality during the acquisition. The GEM GSM-19 station magnetometer data were recorded once every 3 seconds. The CPU clock of the base magnetometer and the helicopter magnetometer were both synchronized to UTC (Universal Time Coordinates) through the built-in GPS receiver to allow correction of diurnals.

Navigation system uses GPS/GLONASS satellite tracking systems to provide real-time WGS-84 coordinate locations for every second. The accuracy achieved with no differential corrections is reported to be $\pm$ 5 meters in the horizontal directions. The GPS receiver antenna was mounted internally inside the canopy of the helicopter.

For quality control, the electromagnetic, magnetic, and radiometric, altitude and navigation data were monitored on four separate windows in the operator's display during flight while they were recorded in three data ASCII streams to the PC hard disk drive. The radiometric data were also recorded to an internal hard drive of the

spectrometer. The data files were transferred to the field workstation via USB flash drive. The raw data files were backed up onto USB flash drive in the field.

2.2 Airborne Survey Instrumentation

Instrument specifications are given in Table 2. Frequencies and coil configuration for the Hummingbird EM system are given in Table 3.

Table 2. Instrument Specifications

Instrument	Producer/Model	Accuracy / Sensitivity	Sampling frequency / interval
Magnetometer	Scintrex Cs-2	<2.5nT throughout range / 0.0006nT √Hz rms	5 Hz
Base magnetometer	GEM GSM-19	0.1 nT	3 s
Electromagnetic	Geotech Hummingbird	1 – 2 ppm	10 Hz
Gamma spectrometer	Radiation Solutions RSX-5	1024 ch's, 16 litres down, 4 litres up	1 Hz
Radar altimeter	Honeywell/ KRA-10A	± 5 ft 40 – 100 ft ± 5 % 100 – 500 ft ± 7 % 500 – 2500 ft	1 Hz
Pressure/temperature	Honeywell PPT	± 0.03 % FS	1 Hz
Navigation	Topcon GPS-receiver	± 5 meters	1 Hz
Acquisition system	NGU custom software		

Figure 2: Hummingbird system in air.

Table 3. Hummingbird EM system, frequency, and coil configurations

Coils	Frequency	Orientation	Separation
A	7701 Hz	Coaxial	6.30 m
B	6606 Hz	Coplanar	6.30 m
C	980 Hz	Coaxial	6.025 m
D	880 Hz	Coplanar	6.025 m
E	34133 Hz	Coplanar	4.90 m

2.3 Airborne Survey Logistics Summary

A summary of the survey specifications is shown in Table 4.

Table 4. Survey Specifications Summary

Parameter	Specifications
Traverse (survey) line spacing	200 meters
Traverse line direction	W-E (100^{o})
Nominal aircraft ground speed	65-130 km/h
Average aircraft ground speed	106 km/h
Average sensor terrain clearance for the bird	45.7 meters
Average sensor terrain clearance for spectrometer	75.7 meters
Sampling rates:	
Magnetometer	0.2 seconds
Electromagnetic system	0.1 seconds
Spectrometer, GPS, altimeter	1.0 second
Base Magnetometer	3.0 seconds

3. DATA PROCESSING AND PRESENTATION

The data acquisition was done by Frida Mathayo Mrope, Tom Kristiansen and Georgios Tassis while the field data quality control was performed by Marie-Andrée Dumais. The ASCII data files were loaded into three separate Oasis Montaj databases. All three datasets were processed consequently according to processing flow charts shown in Appendix A1, A2 and A3. The collected data were processed at NGU. The magnetic data were processed by Alexandros Stampolidis, Frida Mathayo Mrope and Marie-Andrée Dumais. The electromagnetic data were processed by Frida Mathayo Mrope. The radiometric data were processed by Alexandros Stampolidis.

3.1 Total Field Magnetic Data

At the first stage the raw magnetic data were visually inspected, and spikes were removed manually. Non-linear filter was also applied to the airborne raw data to eliminate short-period spikes. Typically, several corrections must be applied to magnetic data before gridding - heading correction, lag correction and diurnal correction.

Diurnal Corrections

The temporal fluctuations in the magnetic field of the earth affect the total magnetic field readings recorded during the airborne survey. This is commonly referred to as the magnetic diurnal variation. These fluctuations can be effectively removed from the airborne magnetic dataset by using a stationary reference magnetometer that records the magnetic field of the earth simultaneously with the airborne sensor at given short time interval.

Diurnal variation channel was inspected for spikes, and spikes were removed manually if necessary. Magnetic diurnals that were recorded on the base station magnetometer were within the standard NGU specifications during the entire survey (Rønning 2013). Diurnal variations were measured with GEM GSM-19 magnetometer. The base station computer clock was continuously synchronized with GPS clock. The recorded data are merged with the airborne data and the diurnal correction is applied according to equation (1).

$$\mathbf{B}_{Tc} = \mathbf{B}_T + (\overline{B}_B - \mathbf{B}_B), \quad (1)$$

Where:

$\mathbf{B}_{Tc}$ = Corrected airborne total field readings

$\mathbf{B}_T$ = Airborne total field readings

$\overline{B}_B$ = Average datum base level

$\mathbf{B}_B$ = Base station readings

The average datum base level ($\overline{B}_{\mathrm{B}}$) was set to 51843.2 nT.

Corrections for Lag and heading

Neither a lag nor cloverleaf tests were performed before the survey. According to previous reports the lag between logged magnetic data and the corresponding navigational data was 1-2 fids. These values were observed to have negligible effect on the processed results. A heading error for a towed system is usually either very small or non-existent. No lag and heading corrections were applied.

Magnetic data processing, gridding, merging with pre-existing data and presentation

The total field magnetic anomaly data ($\mathbf{B}_{TA}$) were calculated from the total field data ($\mathbf{B}_{Tc}$) after subtracting the International Geomagnetic Reference Field (IGRF) model for the surveyed area (equation 2).

$$\mathbf{B}_{TA} = \mathbf{B}_{Tc} - IGRF \tag{2}$$

IGRF 2020 model was employed in these calculations to deduct the magnetic field which may be resulting from the earth's core.

The total field anomaly data were split into lines and then were gridded using a minimum curvature method with a grid cell size of 50 meters. This cell size is exactly one quarter of the 200 meters average line spacing.

The processing steps of magnetic data presented so far, were performed on point basis. The following steps are performed on grid basis.

The horizontal and vertical gradient along with the tilt derivative of the total magnetic anomaly were calculated from the total magnetic anomaly grid. The magnitude of the horizontal gradient (HG) was calculated according to equation (3).

$$HG = \sqrt{\left(\frac{\partial(B_{TA})}{\partial x}\right)^2 + \left(\frac{\partial(B_{TA})}{\partial y}\right)^2} \tag{3}$$

Where: $\mathbf{B}_{TA}$ is the total field anomaly. The vertical gradient (VG) was calculated by applying a vertical derivative convolution filter to the $\mathbf{B}_{TA}$ field. The tilt derivative (TD) was calculated according to equation (4).

$$TD = \tan^{-1}\left(\frac{VG}{HG}\right) \tag{4}$$

The results are presented in a series of coloured shaded relief maps (1:100 000). The maps are:

A. Total field magnetic anomaly
B. Horizontal gradient of total magnetic anomaly
C. Vertical gradient of total magnetic anomaly
D. Tilt derivative (or Tilt angle) of the total magnetic anomaly

These maps are representative of the distribution of magnetization over the surveyed areas. The list of the produced maps is shown in Table 6.

3.2 Electromagnetic Data

The electromagnetic system transmits five fixed frequencies and records an in-phase and a quadrature response for each of the four coil sets of the electromagnetic system. The received signals are processed and used for computation of an apparent resistivity.

To remove the effects of instrument drift caused by gradual temperature variations in the transmitting and receiving circuits, background responses are recorded during each flight. To obtain a background level, the bird is raised to an altitude of at least 1000 ft above the topographic surface so that no electromagnetic responses from the ground are present in the recorded traces. The electromagnetic traces observed at this altitude correspond to a background (zero) level of the system. If these background levels are recorded at 20-30 minutes intervals, then the drift of the system (assumed to be linear) can be removed from the data by resetting these points to the initial zero level of the system. The drift must be removed on a flight-by-flight basis before any further processing is carried out. Geosoft HEM module was used for applying drift correction. Residual instrumental drift, usually small, but non-linear, was manually removed.

When the levelling of the electromagnetic data was completed, in-phase (IP) and quadrature (Q) data were filtered with 10 fiducial non-linear filter to eliminate spherical spikes, which were represented as irregular noise of large amplitude in records and high frequency noise of bird electronics. Then, a 15-fiducial low-pass filter was applied to suppress instrumental and cultural noise. These filters were not able to suppress all the noise completely, due to the irregular nature of noise. Also, shifts of IP and Q records with amplitude of 5-10 ppm was observed in some flights. Shifts were edited manually where possible.

The apparent resistivity was calculated from in-phase and quadrature electromagnetic components using a homogeneous half-space model of the earth (Geosoft HEM module) for 7000 Hz, 6600 Hz, 980 Hz, 880 Hz and 34133 Hz. A half space starting model of 1000 ohm-m, a threshold value of 2 ppm and a fractional error of 1% were used for inversion.

Electromagnetic field decays rapidly with the distance (height of the sensors) – as z^{-2} – z^{-5} depending on the shape of the conductors. And, at certain height, signals from the ground sources become comparable with instrumental noise. Levelling errors or precision of levelling can lead sometimes to appearance of artificial resistivity anomalies when data were collected at high instrumental altitude. Application of a threshold value allows excluding such data from an apparent resistivity calculation, though not completely.

Resistivity data were visually inspected; artificial anomalies associated with high altitude measurements were manually removed. Data recorded at the height above 150 meters were considered as non-reliable and removed from presentation. The most prominent noise from power lines were filtered manually.

Calculated apparent resistivity data were gridded at 50 m x 50 m cell size.

3.3 Radiometric data

Airborne gamma-ray spectrometry measures the abundance of Potassium (K), Thorium (eTh), and Uranium (eU) in rocks and weathered materials by detecting gamma-rays emitted due to the natural radioelement decay of these elements. The data analysis method is based on the IAEA recommended method for U, Th and K (International Atomic Energy Agency, 1991; 2003). A short description of the individual processing steps of that methodology as adopted by NGU is given bellow.

Energy windows
The gamma-ray spectra were initially reduced into standard energy windows corresponding to the individual radio-nuclides K, U and Th. Figure 3 shows an example of a gamma-ray spectrum and the corresponding energy windows and radioisotopes (with peak energy in MeV) responsible for the radiation.

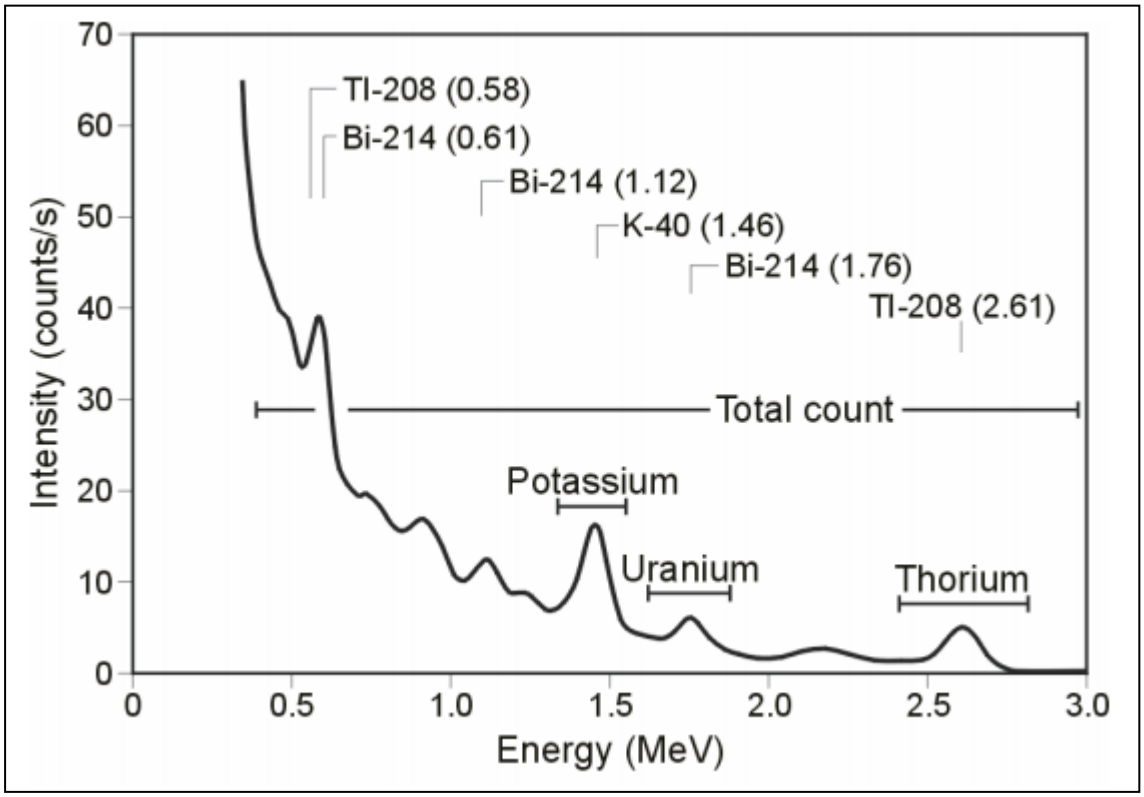

Figure 3: Gamma-ray spectrum with K, Th, U and Total Count windows.

Table 5. Specified channel windows for the 1024 RSX-5 system.

Gamma-ray spectrum	Cosmic	Total count	K	U	Th
Down	1023	137-937	457-523	553-620	803-937
Up	1023			553-620	
Energy windows (MeV)	>3.07	0.41-2.81	1.37-1.57	1.66-1.86	2.41-2.81

The RSX-5 is a 1024 channel system with four downward and one upward looking detector, which means that the actual gamma-ray spectrum is divided into 1024 channels. The first channel is reserved for the “Live Time” and the last for the Cosmic rays. Table 5 shows the channels that were used for the windowing of the spectrum.

Live Time correction

The data were corrected for live time. “Live time” is an expression of the relative length of time the instrument was able to register new pulses per sample interval. On the other hand, “dead time” is an expression of the relative length of time the system was unable to register new pulses per sample interval. The relation between “dead time” and “live time” is given by the equation (5)

$$Live\ time = Real\ time - Dead\ time \tag{5}$$

where the “real time” or “acquisition time” is the elapsed time over which the spectrum is accumulated (about 1 second).

The live time correction is applied to the total count, Potassium, Uranium, Thorium, upward Uranium, and cosmic windows. The formula used to apply the correction is as follows:

$$C_{LT} = C_{RAW} \cdot \frac{Acquisition\ time}{Live\ time} \tag{6}$$

where C_{LT} is the live time corrected channel in counts per second, C_{RAW} is the raw window data in counts per second, while Acquisition time and Live time are in microseconds.

Cosmic and aircraft correction

Background radiation resulting from cosmic rays and aircraft contamination was removed from the total count, Potassium, Uranium, Thorium, upward Uranium windows using the following formula:

$$C_{CA} = C_{LT} - (a_c + b_c \cdot C_{Cos}) \tag{7}$$

where C_{CA} is the cosmic and aircraft corrected window, C_{LT} is the live time corrected window a_c is the aircraft background for this window, b_c is the cosmic stripping coefficient for this window and C_{Cos} is the low pass filtered cosmic window.

Radon correction

The upward detector method, as discussed in IAEA (1991), was applied to remove the effects of the atmospheric radon in the air below and around the helicopter. Using spectrometry data over-water, where there is no contribution from the ground sources, enables the calculation of the coefficients (a_C and b_C) for the linear equations that relate the cosmic corrected counts per second of Uranium channel with that of total count, Potassium, Thorium and Uranium upward channels over water. Data over-land was used in conjunction with data over-water to calculate the a_1 and a_2 coefficients used in equation (8) for the determination of the Radon component in the downward uranium window:

$$Radon_U = \frac{Uup_{CA} - a_1 \cdot U_{CA} - a_2 \cdot Th_{CA} + a_2 \cdot b_{Th} - b_U}{a_U - a_1 - a_2 \cdot a_{Th}} \tag{8}$$

where $Radon_u$ is the radon component in the downward Uranium window, Uup_{CA} is the filtered upward uranium, U_{CA} is the filtered Uranium, Th_{CA} is the filtered Thorium, a_1, a_2, a_U and a_{Th} are proportional factors and b_U an b_{Th} are constants determined experimentally.

The effects of radon in the downward Uranium window are removed by simply subtracting $Radon_U$ from U_{CA}. The effects of radon in the other windows are removed using the following formula:

$$C_{RC} = C_{CA} - (a_C \cdot Radon_U + b_C) \quad (9)$$

where C_{RC} is the Radon corrected window, C_{CA} is the cosmic and aircraft corrected window, $Radon_U$ is the Radon component in the downward uranium window, a_C is the proportionality factor and b_C is the constant determined experimentally for this window from over-water data.

Compton Stripping

Radon corrected Potassium, Uranium and Thorium windows, are subjected to spectral overlap correction. Compton scattered gamma rays in the radio-nuclides energy windows were corrected by window stripping using Compton stripping coefficients determined from measurements on calibrations pads (Grasty et al, 1991) at the Geological Survey of Norway in Trondheim (see values in Appendix A2).

The stripping corrections are given by the following formulas:

$$A_1 = 1 - (g \cdot \gamma) - (a \cdot \alpha) + (a \cdot g \cdot \beta) - (b \cdot \beta) + (b \cdot \alpha \cdot \gamma) \quad (10)$$

$$U_{ST} = \frac{Th_{RC} \cdot ((g \cdot \beta) - \alpha) + U_{RC} \cdot (1 - b \cdot \beta) + K_{RC} \cdot ((b \cdot \alpha) - g)}{A_1} \quad (11)$$

$$Th_{ST} = \frac{Th_{RC} \cdot (1 - (g \cdot \gamma)) + U_{RC} \cdot (b \cdot \gamma - a) + K_{RC} \cdot ((a \cdot g) - b)}{A_1} \quad (12)$$

$$K_{ST} = \frac{Th_{RC} \cdot ((\alpha \cdot \gamma) - \beta) + U_{RC} \cdot ((a \cdot \beta) - \gamma) + K_{RC} \cdot (1 - (a \cdot \alpha))}{A_1} \quad (13)$$

where U_{RC}, Th_{RC}, K_{RC} are the radon corrected Uranium, Thorium and Potassium and a, b, g, α, β, γ are Compton stripping coefficients. U_{ST}, Th_{ST} and K_{ST} are stripped values of U, Th and K.

Reduction to Standard Temperature and Pressure

The radar altimeter data were converted to effective height (H_{STP}) using the acquired temperature and pressure data, according to the expression:

$$H_{STP} = H \cdot \frac{273.15}{T + 273.15} \cdot \frac{P}{1013.25} \quad (14)$$

where H is the smoothed observed radar altitude in meters, T is the measured air temperature in degrees Celsius and P is the measured barometric pressure in millibars.

Height correction
Variations caused by changes in the aircraft altitude relative to the ground was corrected to a nominal height of 60 m. Data recorded at the height above 150 m were considered as non-reliable and removed from processing. Total count, Uranium, Thorium and Potassium stripped windows were subjected to height correction according to the equation:

$$C_{60m} = C_{ST} \cdot e^{C_{ht} \cdot (60 - H_{STP})} \quad (15)$$

where C_{ST} is the stripped corrected window, C_{ht} is the height attenuation factor for that window and H_{STP} is the effective height.

Conversion to ground concentrations
Finally, corrected count rates were converted to effective ground element concentrations using calibration values derived from calibration pads (Grasty et al, 1991) at the Geological Survey of Norway in Trondheim (see values in Appendix A2). The corrected data provide an estimate of the apparent surface concentrations of Potassium, Uranium and Thorium (K, eU and eTh). Potassium concentration is expressed as a percentage, equivalent Uranium and Thorium as parts per million (ppm). Uranium and Thorium are described as “equivalent” since their presence is inferred from gamma-ray radiation from daughter elements (^{214}Bi for Uranium, ^{208}TI for Thorium). The concentration of the elements is calculated according to the following expressions:

$$C_{CONC} = C_{60m} / C_{SENS\_60m} \quad (16)$$

where C_{60m} is the height corrected channel, C_{SENS_60m} is experimentally determined sensitivity reduced to the nominal height (60m).

Spectrometry data gridding and presentation
Gamma-rays from Potassium, Thorium and Uranium emanate from the uppermost 30 to 40 cm of soil and bedrock (Minty, 1997). Variations in the concentrations of these radioactive elements are largely related to changes in the mineralogy and geochemistry of the Earth’s surface.

The spectrometry data were stored in a database and the ground concentrations were calculated following the processing steps. A list of the parameters used in these steps is given in Appendix A3.

Then the data were split in lines and ground concentrations of the three main natural radio-elements Potassium, Thorium and Uranium and total gamma-ray flux (total count) were gridded using a minimum curvature method with a grid cell size of 50 meters, as in the case of the magnetic data. The quality of the radiometric data was within standard NGU specifications (Rønning 2013). For further reading regarding standard processing of airborne radiometric data, we recommend the publications from Minty et al. (1997).

A 3x3 convolution filter was applied to smooth the concentration grids before the creation of the ternary map. A list of the produced maps is shown on Table 6.

4. PRODUCTS

Processed digital data from the survey are presented as:

1. Geosoft XYZ files:
   Trøndelag_2021_EM.xyz,
   Trøndelag_2021_Magnetometry.xyz,
   Trøndelag_2021_Radiometry.xyz

   Coloured maps at the scale 1:100 000 available from NGU on request.

2. Grid-files in Geosoft grid format

Table 6. Maps available from NGU on request.

Map #	Name
2022.008-00	Survey Flight Path
2022.008-01	Total magnetic field
2022.008-02	Magnetic Horizontal Gradient
2022.008-03	Magnetic Vertical Gradient
2022.008-04	Magnetic Tilt Derivative
2022.008-05	Apparent resistivity, Frequency 7000 Hz, coaxial coils
2022.008-06	Apparent resistivity, Frequency 6600 Hz, coplanar coils
2022.008-07	Apparent resistivity, Frequency 980 Hz, coaxial coils
2022.008-08	Apparent resistivity, Frequency 880 Hz, coplanar coils
2022.008-09	Apparent resistivity, Frequency 34133 Hz, coplanar coils
2022.008-10	Apparent resistivity, Frequency 4551 Hz, coaxial coils *
2022.008-11	Apparent resistivity, Frequency 4287 Hz, coplanar coils *
2022.008-12	Apparent resistivity, Frequency 923 Hz, coaxial coils *
2022.008-13	Apparent resistivity, Frequency 32165 Hz, coplanar coils *
2022.008-14	Radiometric Total counts
2022.008-15	Potassium ground concentration
2022.008-16	Uranium ground concentration
2022.008-17	Thorium ground concentration
2022.008-18	Radiometric Ternary Map

Downscaled images of the maps are shown on Figure 4 to Figure 18. Maps are presented with a scale of 1:100 000.

5. REFERENCES

IAEA 1991: Airborne Gamma-Ray Spectrometry Surveying, Technical Report No 323, Vienna, Austria, 97 pp

Geotech 1997: Hummingbird Electromagnetic System. User manual. Geotech Ltd. October 1997

Grasty, R.L., Holman, P.B. & Blanchard 1991: Transportable Calibration pads for ground and airborne Gamma-ray Spectrometers. Geological Survey of Canada. Paper 90-23. 62 pp.

IAEA 2003: Guidelines for radioelement mapping using gamma ray spectrometry data. IAEA-TECDOC-1363, Vienna, Austria. 173 pp.

Minty, B.R.S., Luyendyk, A.P.J. and Brodie, R.C. 1997: Calibration and data processing for gamma-ray spectrometry. AGSO – Journal of Australian Geology & Geophysics. 17(2). 51-62.

Naudy, H. and Dreyer, H. 1968: Non-linear filtering applied to aeromagnetic profiles. Geophysical Prospecting. 16(2). 171-178.

Rønning, J.S. 2013: NGUs helikoptermålinger. Plan for sikring og kontroll av datakvalitet. NGU Intern rapport 2013.001, (38 sider).

Appendix A1: Flow chart of magnetic processing

Meaning of parameters is described in the referenced literature.

Processing flow:

- Quality control
- Visual inspection of airborne data and manual spike removal
- Import of diurnal data
- Correction of data for diurnal variation
- IGRF removed
- Splitting flight data by lines
- Gridding

Appendix A2: Flow chart of EM processing

Meaning of parameters is described in the referenced literature.

Processing flow:

- Automated leveling using Geosoft HEM module
- Filtering of in-phase and quadrature channels with non-linear and low-pass filters
- Quality control and visual inspection of data
- Manual removal of remaining part of instrumental drift
- Calculation of an apparent resistivity using in-phase and quadrature channels
- Splitting flight data by lines
- Gridding

Appendix A3: Flow chart of radiometry processing

Underlined processing stages are not only applied to the K, U and Th window, but also to the total count.
Meaning of parameters is described in the referenced literature.

- Airborne and cosmic correction (IAEA, 2003)
  Used parameters: determined by high altitude calibration flights (1500-9000 ft) at Randsfjorden in 2021.

Channel	Background	Cosmic
K	6.5274	0.0537
U	4.3312	0.0373
Th	0	0.0694
Uup	1.1423	0.0108
Total counts	71.552	0.936

- Radon correction using upward detector method (IAEA, 2003)
  Used parameters determined from survey data over water and land (Kjøkkenbukta and Gjetardalstinden), August 2021:

Coefficient	Value	Coefficient	Value
a_u	0.94545	b_u	0
a_K	6.09545	b_K	0
a_{Th}	0.52727	b_{Th}	0.33273
a_{TC}	60.53182	b_{TC}	0
a_1	0.04314902	a_2	0.03066187

- Stripping corrections (IAEA, 2003)

Used parameters determined from measurements on calibrations pads at NGU, May 2021

Coefficient	Value
a	0.048987
b	0
c	0
α	0.302131
β	0.463789
γ	0.795178

- Height correction to a height of 60 m
  Parameters determined by high altitude calibration flights (100 – 700 ft). The average values from tests performed at Randsfjorden, 2021 were used. Attenuation factors in 1/m:

Channel	Attenuation factor
K	-0.0103
U	-0.0093
Th	-0.0085
TC	-0.0088

- Converting counts at 60 m heights to element concentration on the ground
  Used parameters determined from measurements on calibrations pads at NGU, May 2021

Channel	Sensitivity
K (%/count)	0.00731
U (ppm/count)	0.08489
Th (ppm/count)	0.15411

- Gridding

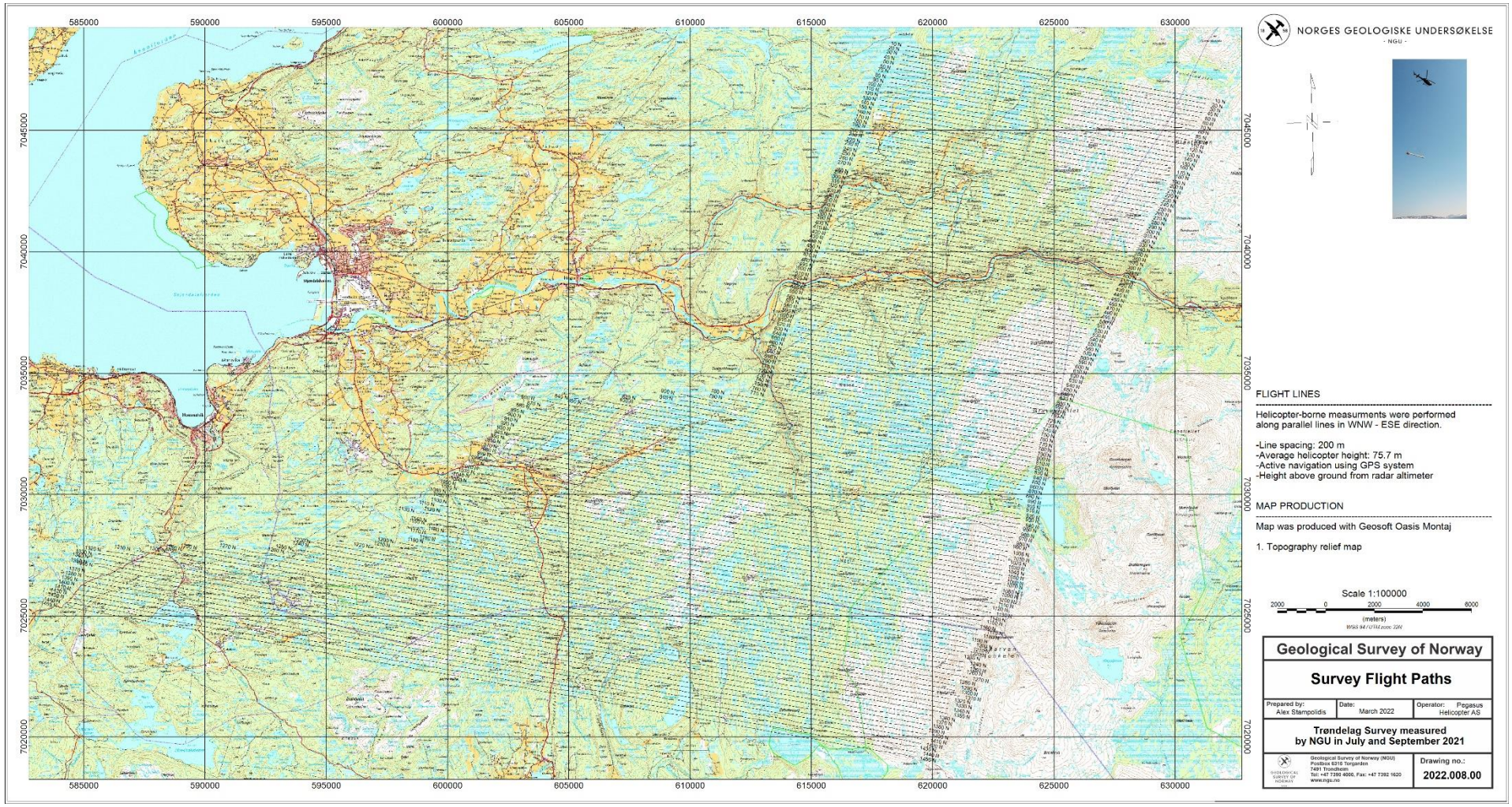

Figure 4: Trøndelag survey area with flight paths.

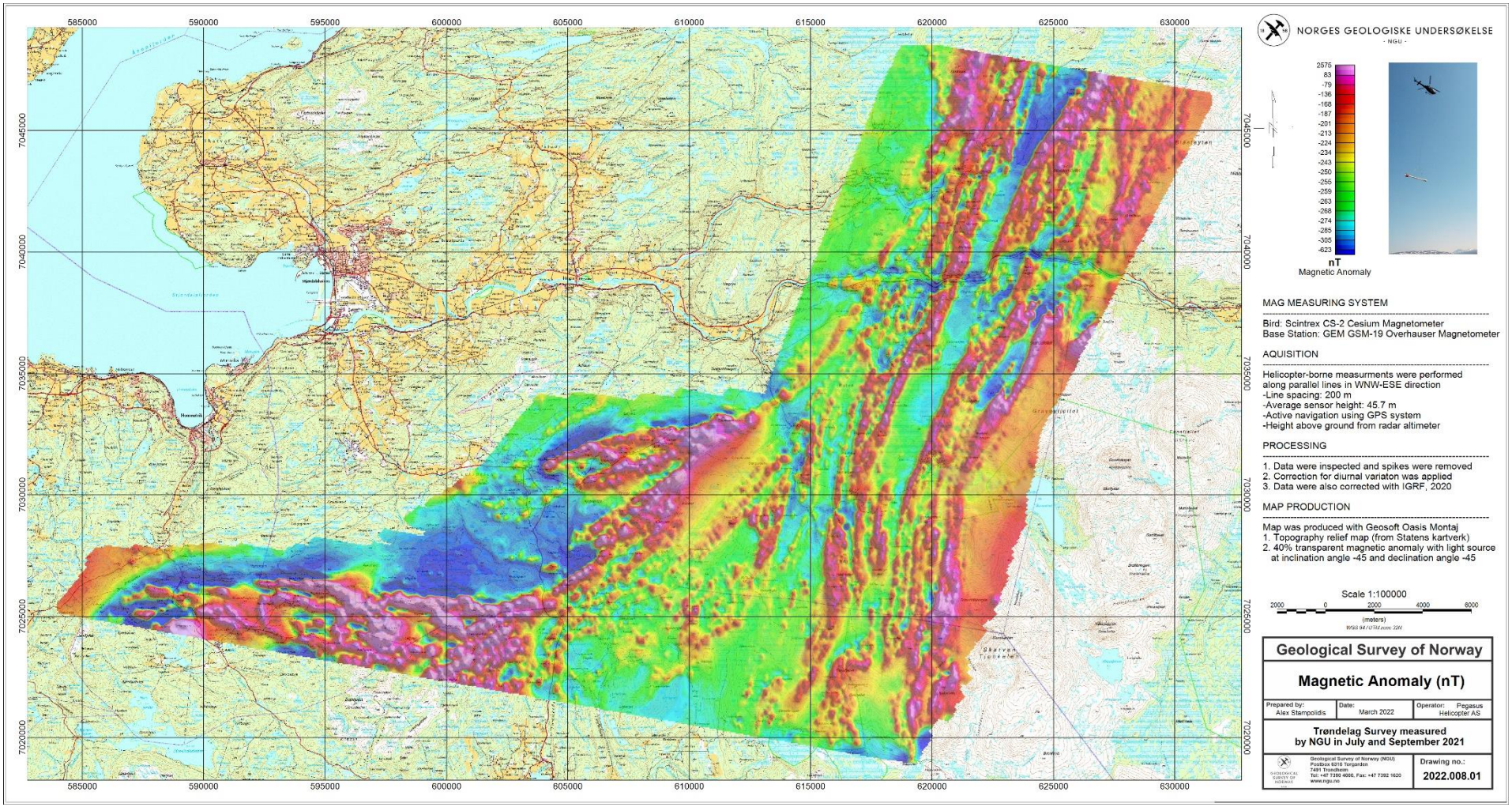

Figure 5: Total Magnetic Field.

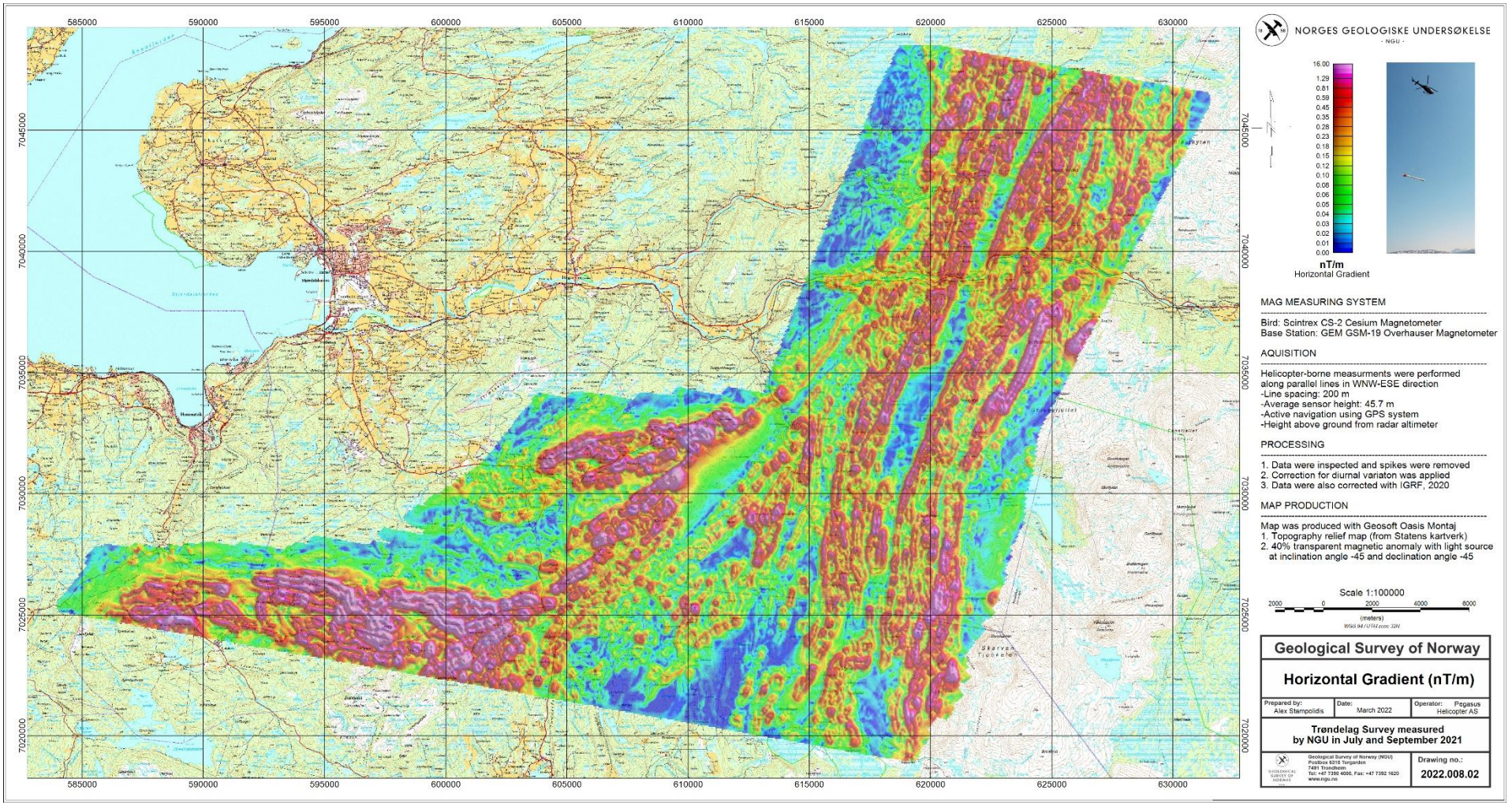

Figure 6: Magnetic Horizontal Gradient.

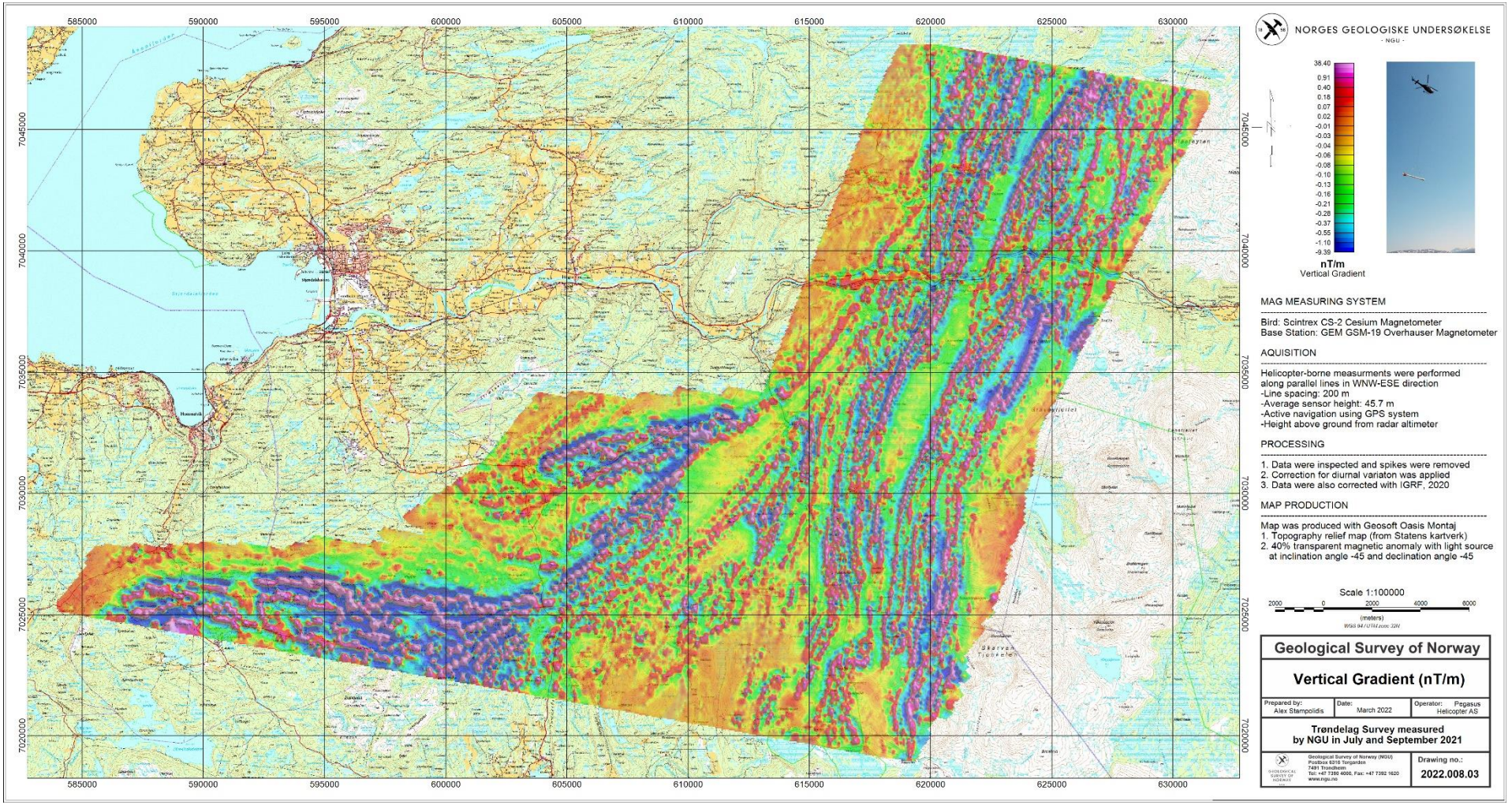

Figure 7: Magnetic Vertical Gradient.

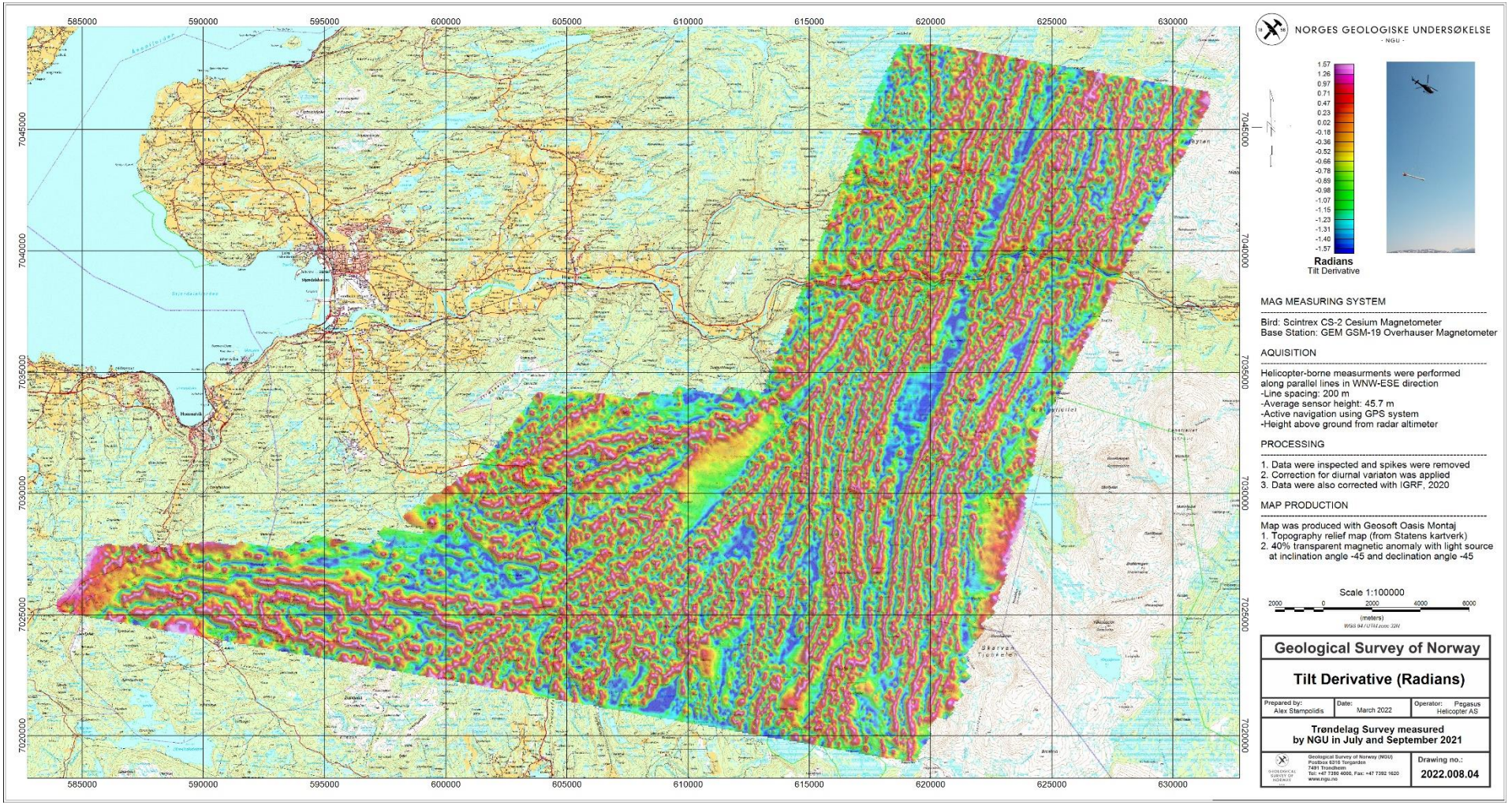

Figure 8: Magnetic Tilt Derivative.

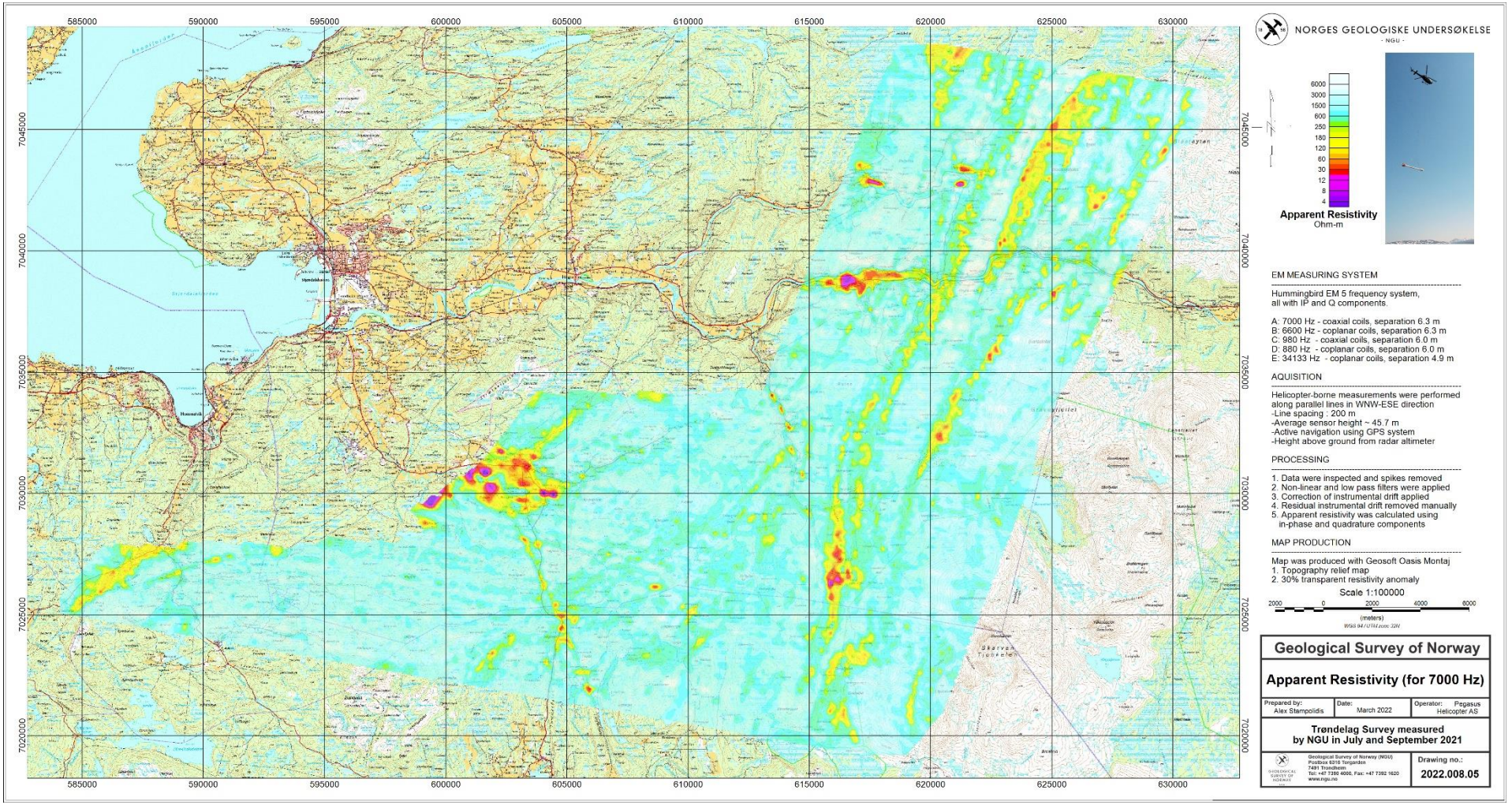

Figure 9: Apparent resistivity. Frequency 7000 Hz, Coaxial coils.

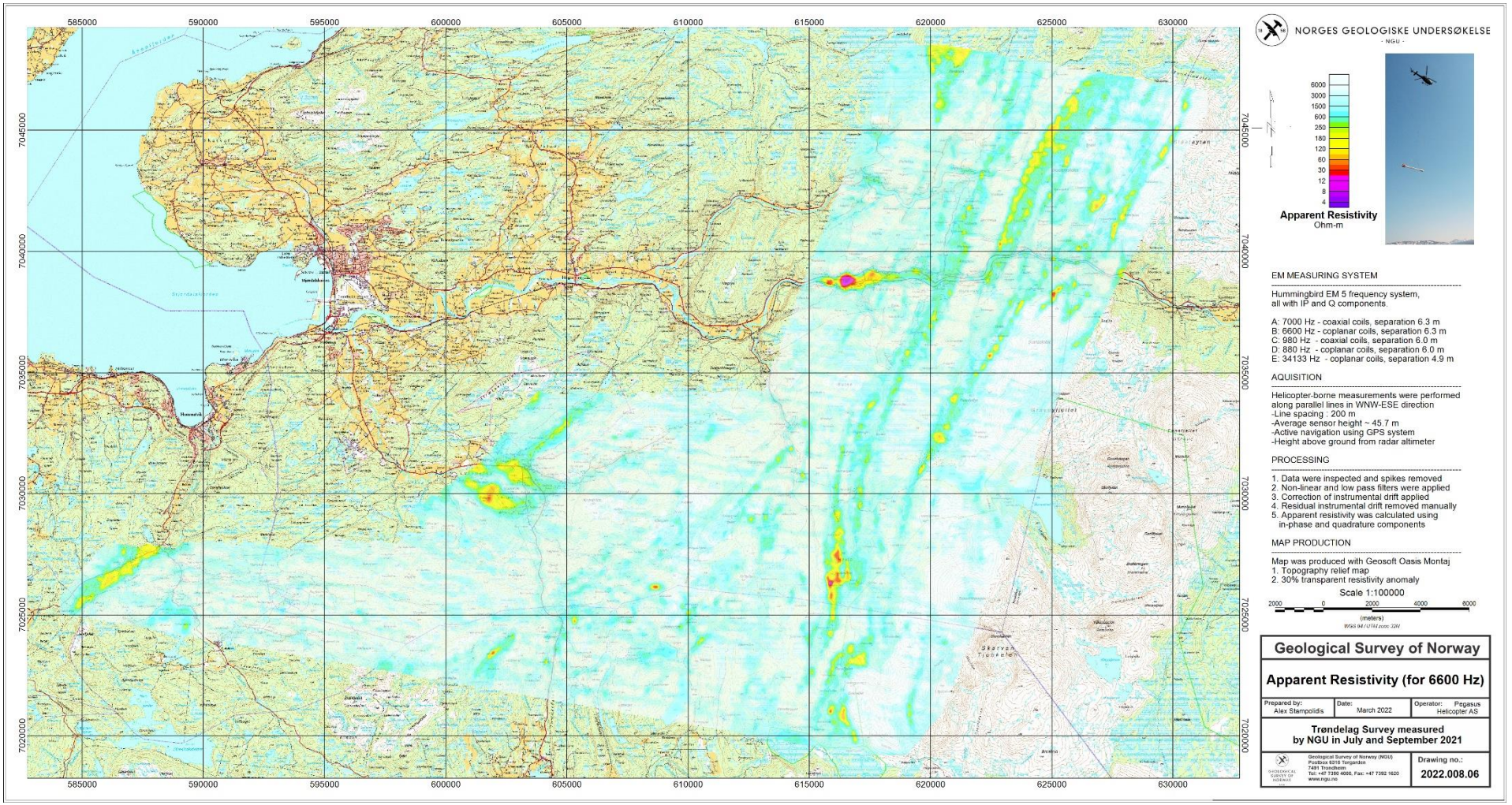

Figure 10: Apparent resistivity. Frequency 6600 Hz, Coplanar coils.

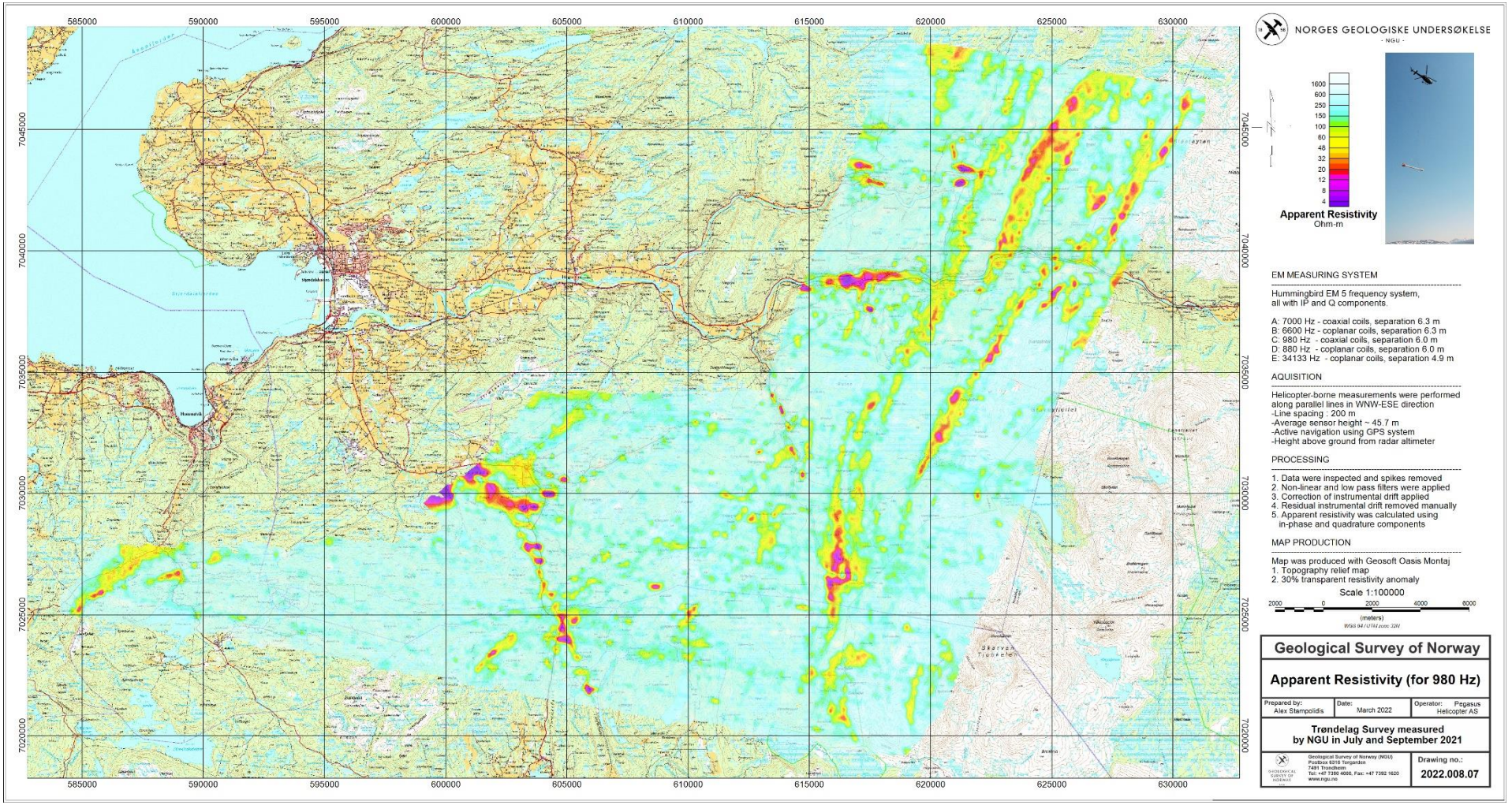

Figure 11: Apparent resistivity. Frequency 980 Hz, Coaxial coils.

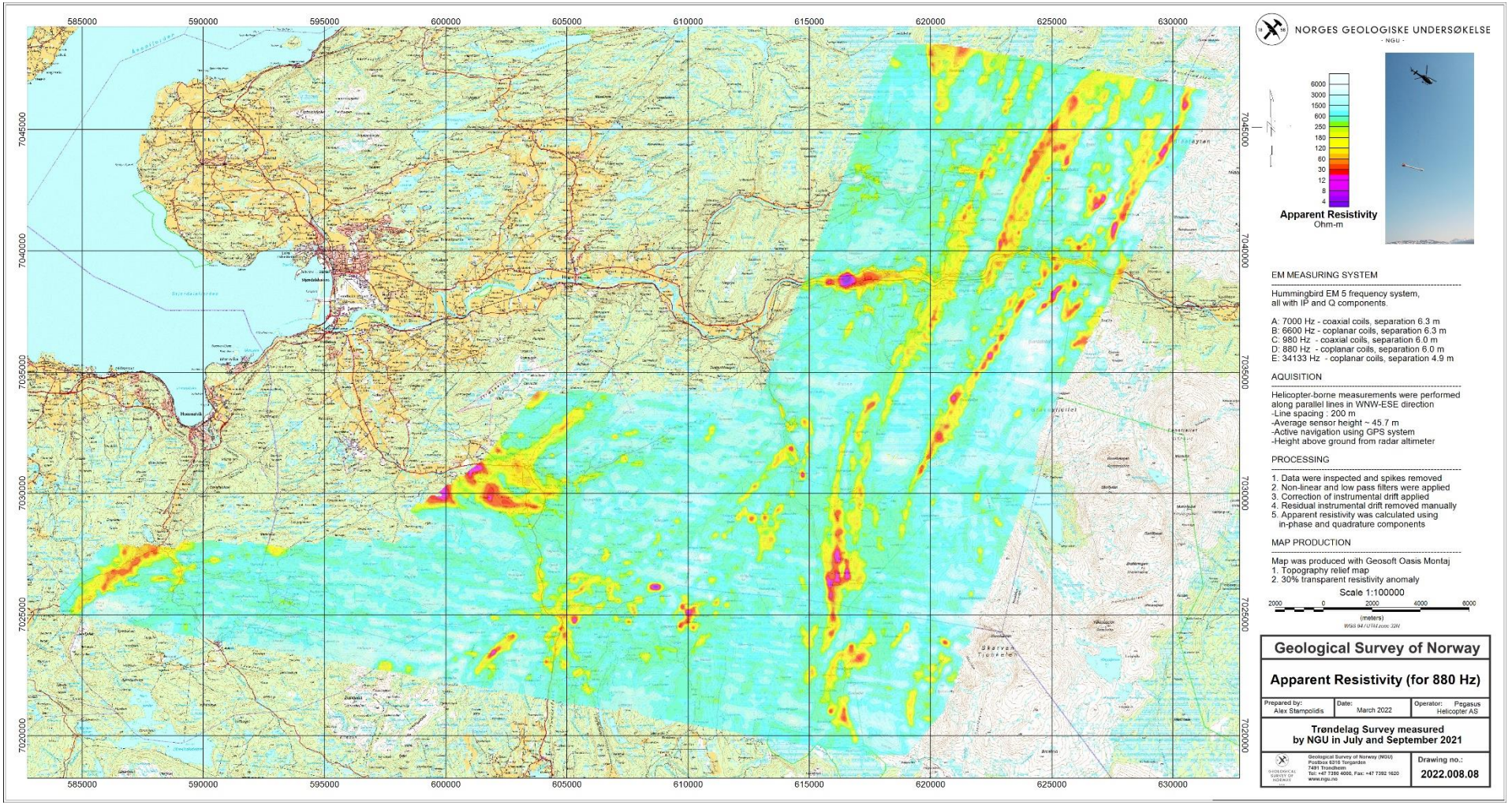

Figure 12: Apparent resistivity. Frequency 880 Hz, Coplanar coils.

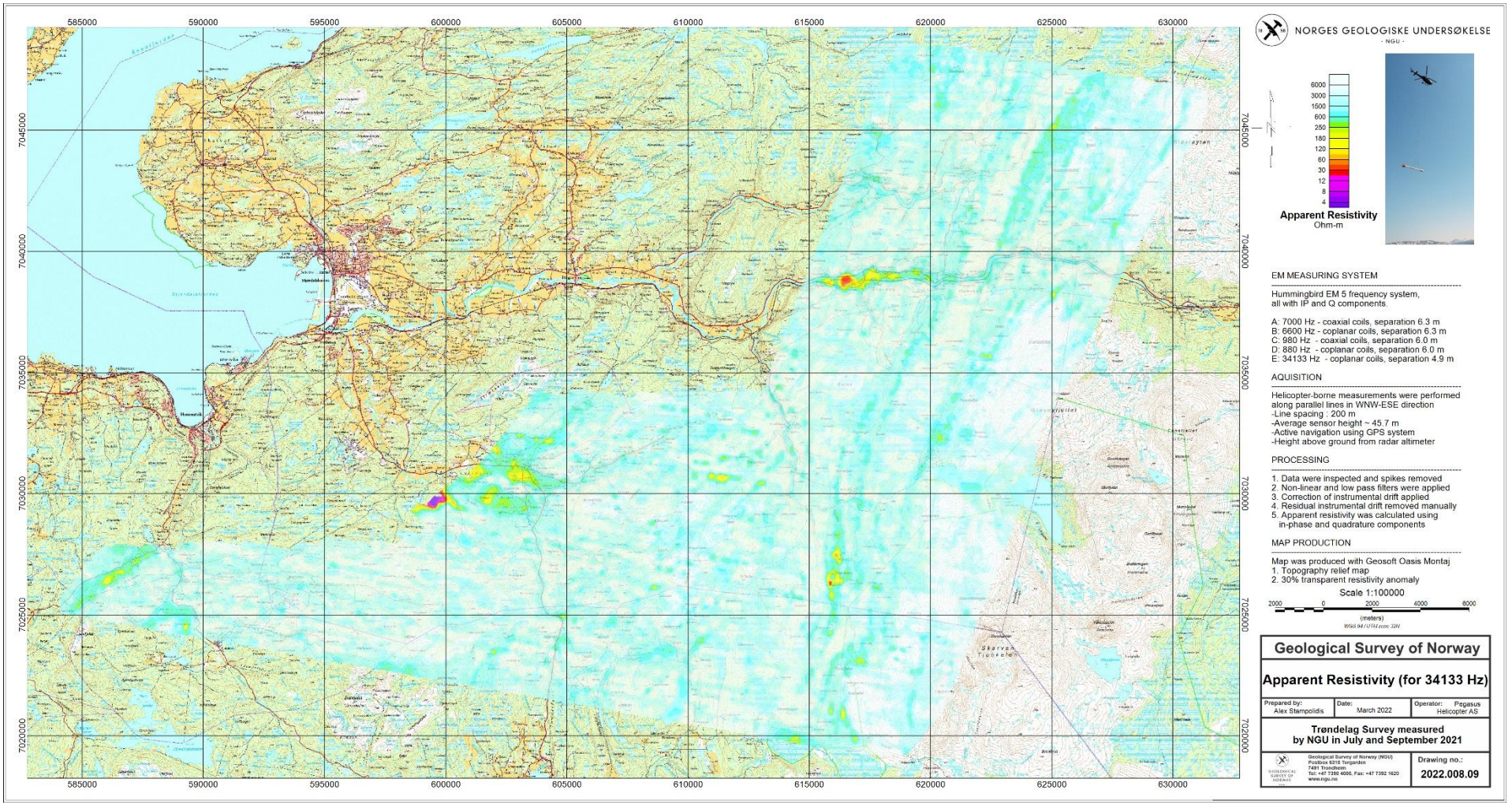

Figure 13 Apparent resistivity. Frequency 34133 Hz, Coplanar coils.

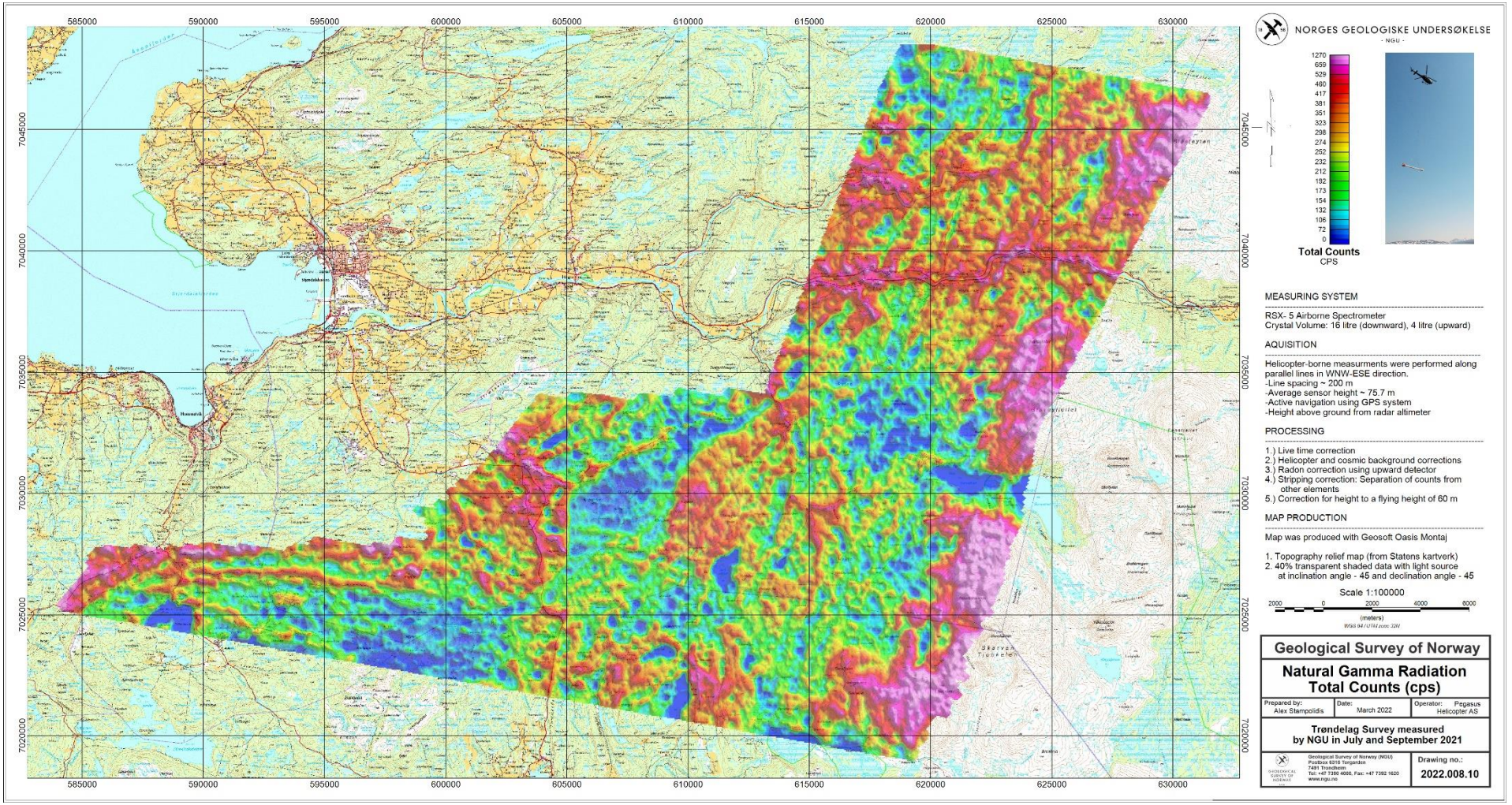

Figure 14: Radiometric Total counts.

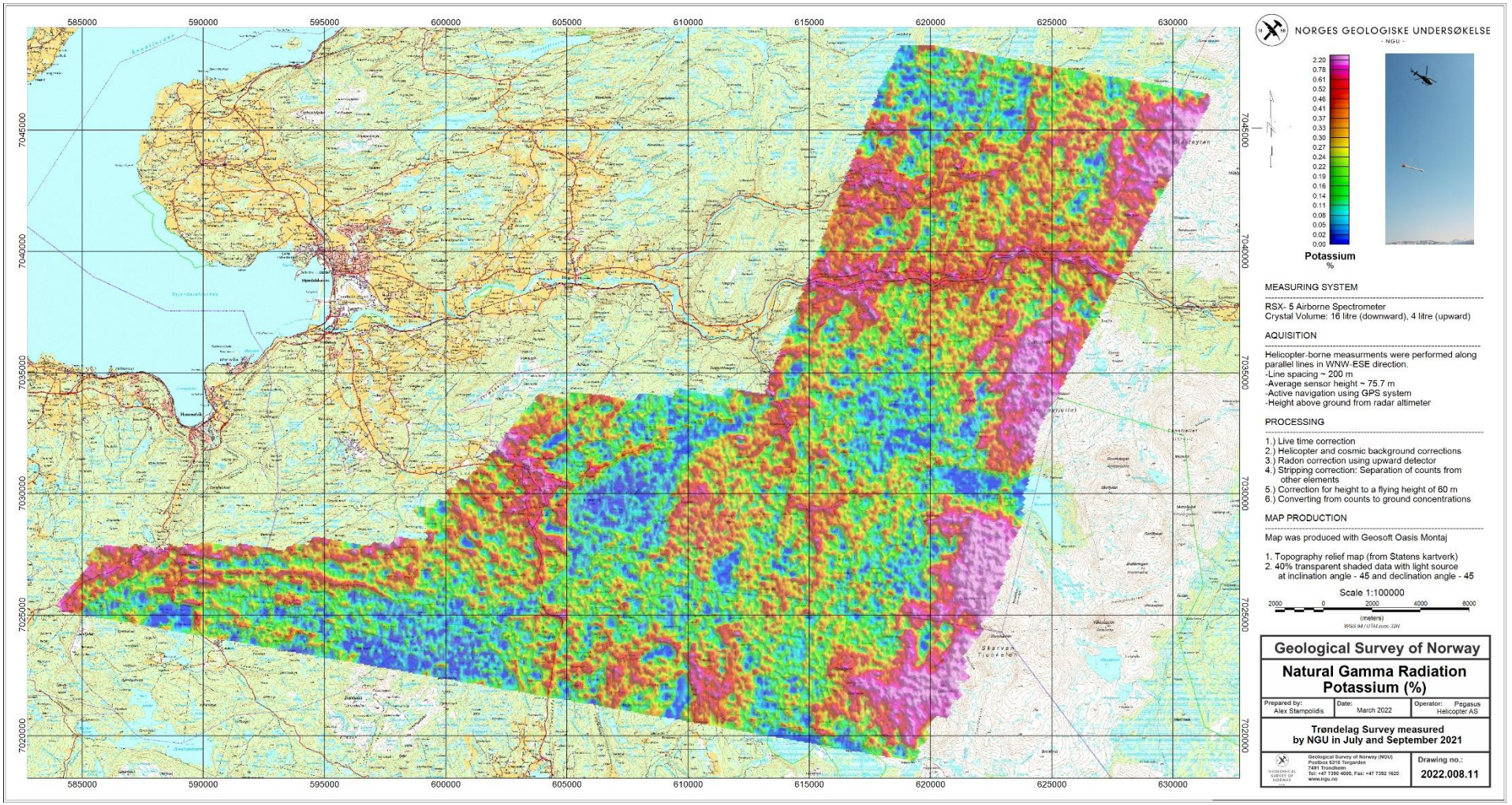

Figure 15: Potassium ground concentration.

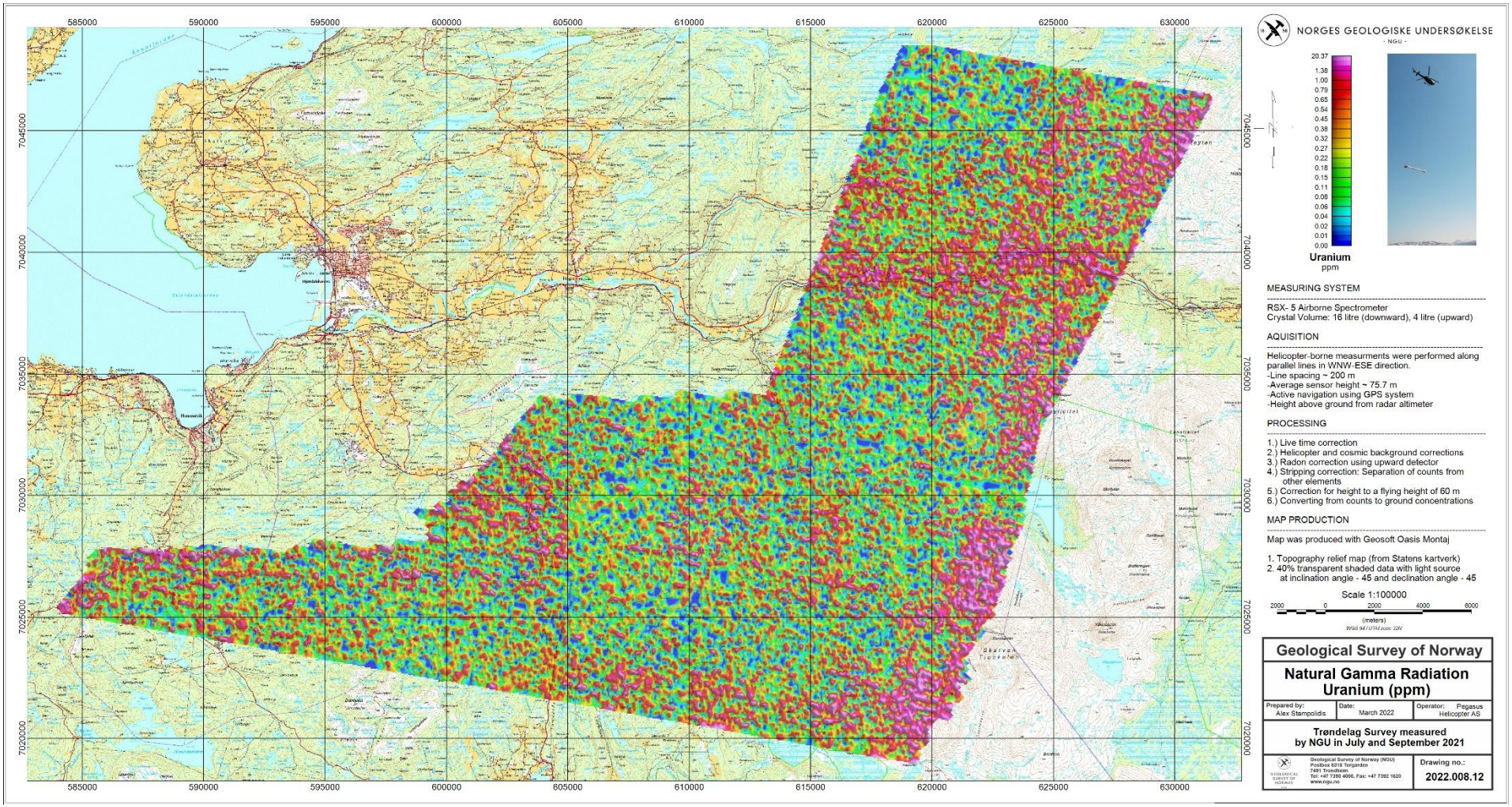

Figure 16: Uranium ground concentration.

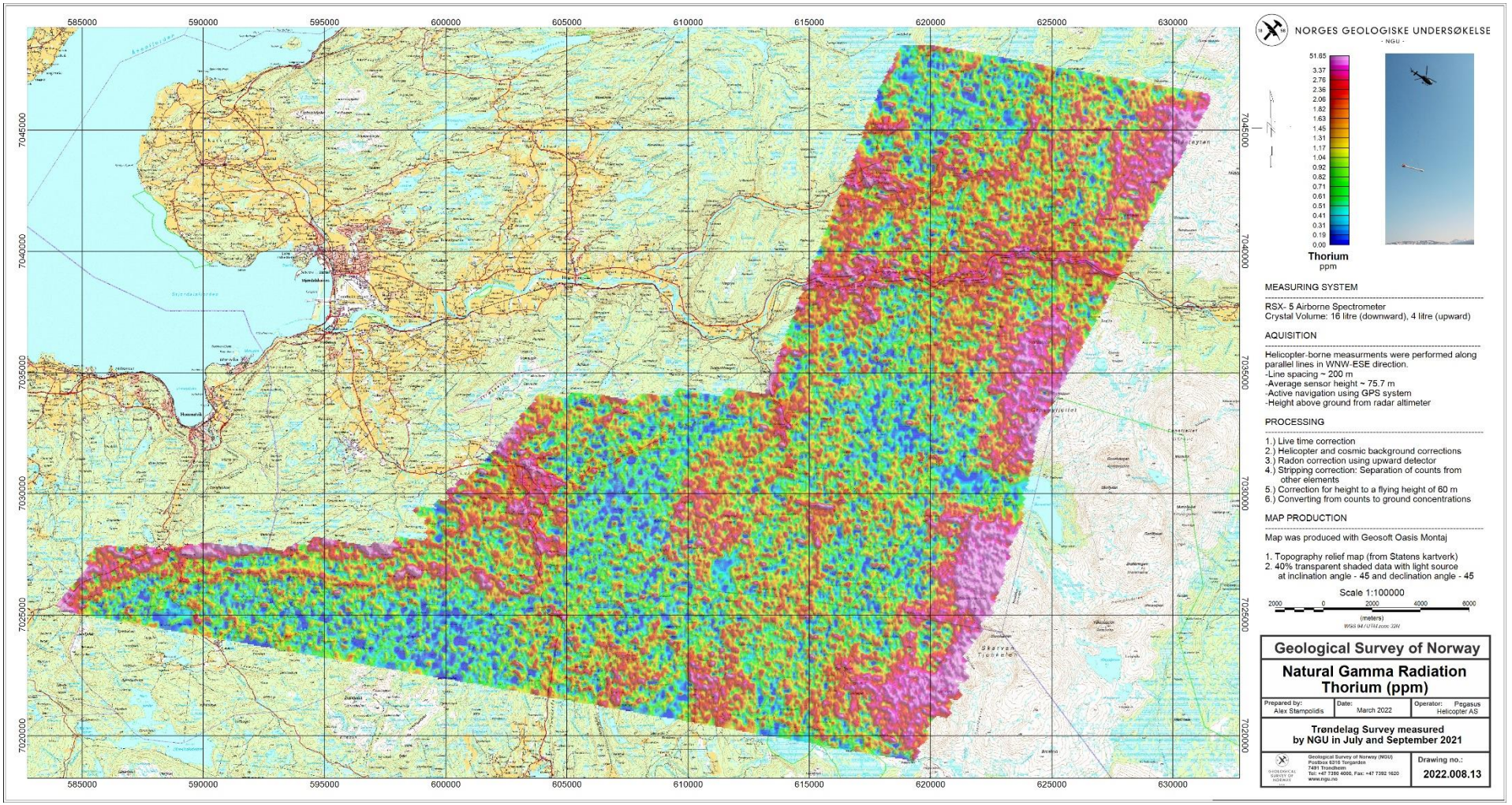

Figure 17: Thorium ground concentration.

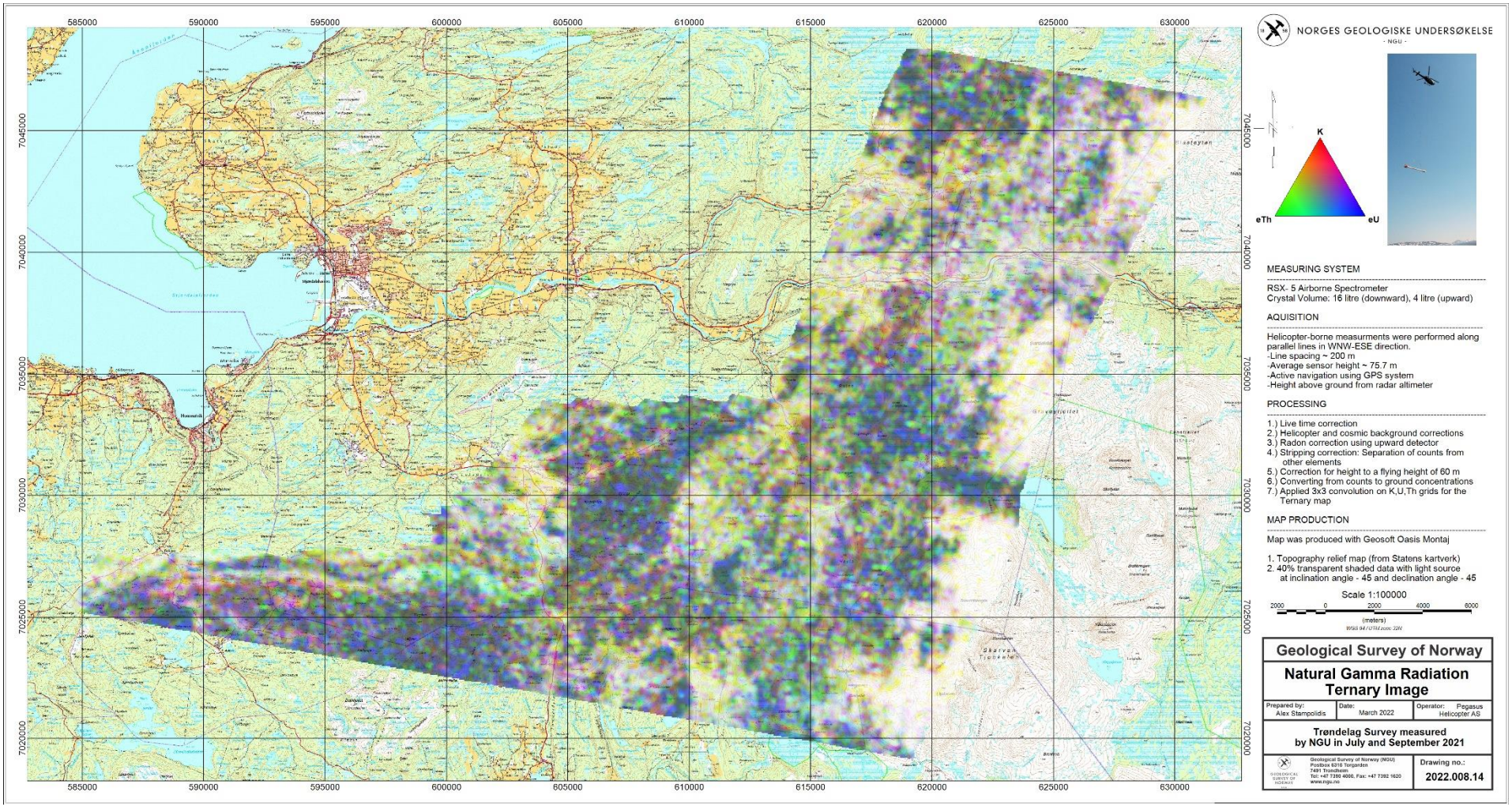

Figure 18: Radiometric Ternary Image.

GEOLOGICAL
SURVEY OF
NORWAY

· NGU ·

Geological Survey of Norway
PO Box 6315, Sluppen
N-7491 Trondheim, Norway

Visitor address
Leiv Eirikssons vei 39
7040 Trondheim

Tel (+ 47) 73 90 40 00
E-mail ngu@ngu.no
Web www.ngu.no/en-gb/